ChemPubSoc Europe

DOI: 10.1002/cctc.201900519

CHEMCATCHEM Full Papers

The Role of Brønsted and Water-Tolerant Lewis Acid Sites in the Cascade Aqueous-Phase Reaction of Triose to Lactic Acid

Kryslaine M. A. Santos,[a] Elise M. Albuquerque,[b] Giada Innocenti,[c, d, e] Luiz E. P. Borges,[a] Carsten Sievers,[c] and Marco A. Fraga*[a, b]

Aqueous-phase conversion of glyceraldehyde to lactic acid was investigated over Nb_2O_5, TiO_2, ZrO_2 and SnO_2 in a fixed-bed up-flow reactor. Special attention was given to the catalysts acidity regarding the type, amount, strength and tolerance to water of surface acid sites. These sites were assessed by infrared spectroscopy of pyridine adsorbed on dehydrated and hydrated catalysts as well as by isopropanol decomposition. It was found that Nb_2O_5 and TiO_2 have the highest fraction of water-tolerant Lewis acid sites (40 and 47%), while only 6% was estimated for ZrO_2. No relevant Lewis acidity was observed on SnO_2, but it was noticed the presence of strong base sites. The transformation of glyceraldehyde into lactic acid proceeded via a cascade reaction in which glyceraldehyde is firstly dehydrated to pyruvaldehyde, followed by its rearrangement to lactic acid with the addition of a water molecule. The dehydration step occurs on Brønsted acid sites and/or on water-tolerant Lewis acid sites. These latter sites also determine the selectivity to lactic acid. Strong base sites promote glyceraldehyde fragmentation leading to formaldehyde with high selectivity.

Introduction

Environmental problems caused by human intervention have been increasingly gained attention. A lot of effort has been made to minimize these problems by reducing greenhouse gases emissions, controlling environmental reserves depletion, and reducing and remediating of environmental pollution. In this pursuit, the use of biomass to generate biofuels and bio-based chemicals is attracting much interest since processing renewable feedstocks can be sustainable and environment-friendly, paving the way to a green economy within the concept of a biorefinery.[1]

Among all sort of available biomass, such as triglycerides, terpenes, carbohydrates and lignin, triglycerides are convenient compounds since their use is attainable in the industry for fuel and chemical production in a shorter term.[2] Indeed, the production of biodiesel from triglyceride by transesterification increased significantly in the past few years.[3] Biodiesel is biodegradable, presents low toxicity and is less polluting than petrodiesel.[4,5] Along with biodiesel, glycerol is formed as a by-product, corresponding to about 10% of the total volume of the biofuel produced.[6] Such a large co-production, which surpasses the current industrial consumption for the conventional end-use applications, makes glycerol a promising platform molecule that can be converted into value-added products. Different catalytic transformation through dehydrogenation,[7] oxidation,[8] condensation[9] and etherification[10] reactions have indeed been exploited as the base of a glycerol biorefinery.[11,12] Lactic and acrylic acids, diols, allyl alcohols, epichlorohydrin and glycerol carbonate can be listed as the most pertinent glycerol-derivatives chemicals in this scenario.[11,13] Lactic acid (2-hydroxypropanoic acid) stands out mainly because of the rising market of biodegradable poly (lactic acid)[14] and the need for a more robust and alternative process to the current fermentative industrial route.

Different reaction pathways can lead to lactic acid from glycerol either in one-pot or multi-stage processes relying on heterogeneous catalysts. Glycerol can go through hydrogenolysis forming 1,2-propanediol[15] and then be converted into lactic acid by oxidation.[16] It can also be initially dehydrated to acetol over acid catalyst[17] followed by oxidation/Cannizzaro reactions.[18,19] Alternatively, glycerol can be dehydrogenated to trioses[20–22] that are further dehydrated to pyruvaldehyde[23] on acid catalysts, followed by Cannizzaro reaction to lactic acid.[24,25]

[a] K. M. A. Santos, Prof. L. E. P. Borges, Prof. M. A. Fraga
Seção de Química
Instituto Militar de Engenharia
Praça Gen. Tibúrcio, 80, Praia Vermelha, Urca, Rio de Janeiro/RJ 22290-270 (Brazil)
E-mail: marco.fraga@int.gov.br
[b] Dr. E. M. Albuquerque, Prof. M. A. Fraga
Divisão de Catálise e Processos Químicos
Instituto Nacional de Tecnologia/MCTIC
Av. Venezuela, 82/518, Saúde, Rio de Janeiro/RJ 20081-312 (Brazil)
[c] Dr. G. Innocenti, Prof. C. Sievers
School of Chemical & Biomolecular Engineering
Georgia Institute of Technology
311 Ferst Dr. NW., Atlanta, GA 30332-0100 (USA)
[d] Dr. G. Innocenti
Dipartimento di Chimica Industriale "Toso-Montanari"
Università di Bologna
Viale del risorgimento 4, Bologna 40136 (Italy)
[e] Dr. G. Innocenti
Consorzio INSTM
Research Unit of Bologna
Firenze (Italy)

Supporting information for this article is available on the WWW under https://doi.org/10.1002/cctc.201900519

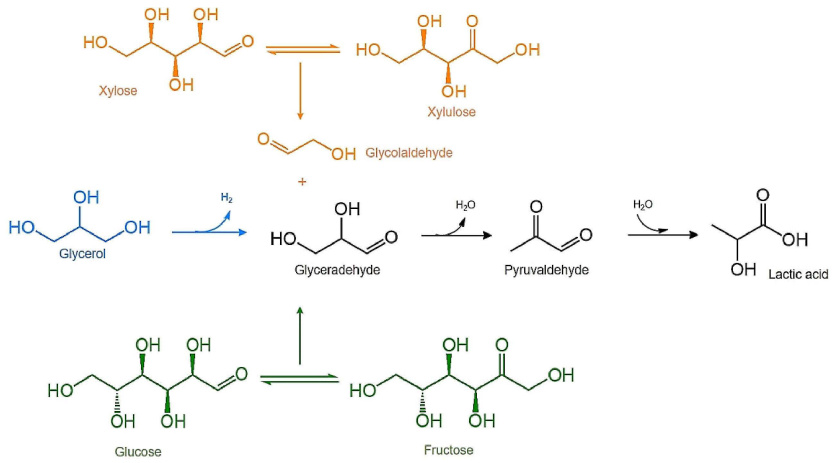

Scheme 1. Pathways to obtain lactic acid from biomass derived molecules.

Catalytic chemical conversion of trioses to lactic acid or alkyl lactates has been drawing large interest over the last years.[26–36] Not only does it add value to biodiesel production chain, but it also opens the way to exploit waste lignocellulose monosaccharides (pentoses and hexoses). In fact, trioses are found as intermediates during the chemocatalytic conversion of pentoses and hexoses to lactic acid via retro-aldol condensation reactions (Scheme 1).[36–42] Therefore, understanding their conversion process also aids to widen alternative green routes to lactic acid production, especially as concerning material supply.

Trioses, glyceraldehyde and dihydroxyacetone, have both been used since they are readily interconvertible via isomerization. Indeed, the same lactic acid yield was reached on Sn-Beta zeolite using either glyceraldehyde or dihydroxyacetone as feedstock.[26] Nonetheless, most studies are limited to the use of alcohols as solvents, which leads to the formation of alkyl lactates.[26–34] The preferable synthesis in alcoholic medium is driven by the higher stability of trioses in alcohol while the formation of carbonaceous deposits is seen in water, leading to catalyst coking.[26,27] Furthermore, strong structural damage has been reported on ordered catalysts when reaction is run in water.[26,27,35,36] As a consequence, a wide number of catalysts, such as zeolites (Y,[27–29] USY,[27–29] ZSM-5,[27,29] Beta[26,27] and Mordenite[27]), substituted zeolites (Zr-,[26] Ti-[26] and Sn-Beta,[26,36] Sn-ZSM-5[30] and Sn-MCM-22[43]), hierarchical zeolites (Sn-[44] and Nb-FAU,[45] Sn-[44] and Nb-BEA[45]), ordered mesoporous substituted-silicates (Al-, Ga- and Sn-MCM-41[31]), montmorillonite,[27,32] sulphated zirconia,[27] ZrO_2–TiO_2 mixed oxide,[33] and alumina-supported SnO_2[34,46,47] have been investigated so far in short-chain alcohols (C1–C4), mostly methanol or ethanol. From these studies, some authors reported that Lewis acid sites[26,27,34] catalyze the production of alkyl lactates from trioses while Brønsted acid sites[26,43] promote the formation of undesired side-products (dialkyl acetals), following a different reaction path, or carbonaceous deposits. Others argued that Lewis acid sites are the ones promoting lactate yields despite recognizing the helpful role of weak Brønsted acid sites in the initial triose dehydration step.[29,31,36] They suggested that only the strong Brønsted acid sites catalyze the formation of alkyl acetals and these sites should thus be avoided in the catalyst formulation. Kinetic and mechanistic studies have also been performed, and the reaction in alcohols was shown to proceed through a complex network. A pseudohomogeneous mechanism and first order rate expressions were reported for obtaining alkyl lactates.[46,47]

There are only a few studies in the literature that used water as solvent to produce lactic acid, and they focused on the performance of zeolites (Y, USY, ZSM-5, Beta and Mordenite),[27] substituted zeolites (Zr-,[26] Ti-[26] and Sn-Beta,[26] and Sn-MCM-22[43]), tin phosphates[48] and carbon–silica composites.[36] These authors concluded that the Lewis acid sites can catalyze the formation of lactic acid from trioses[26,27] and that the catalyst activity was associated with the strength of such sites; the stronger the Lewis acid sites the more active the catalyst.[26]

The well-known susceptibility of Lewis acid sites to water has not been discussed in detail, probably due to the short number of studies concerning aqueous-phase transformations of trioses.[26,27,35,36] Indeed, the lack of a better understanding of the active sites for lactic acid production prevents the development of suitable catalysts for technological applications. Moreover, it should be considered that biomass-derived monosaccharides are generally available in water; therefore, dealing with aqueous-phase reactions is imperative for the establishment of a biorefinery.[49]

Previous studies on the conversion of biomass-derived monosaccharides with water-tolerant Lewis acid catalysts in water or water/organic solvent mixtures have focused on the use of both homogeneous (rare earth triflates[50,51]) and heterogeneous systems, mostly Sn-Beta[26,41] and Nb_2O_5.[35,50,52] Despite the activity of rare earth triflates,[51] heterogeneous catalysts present the additional advantages of being easily recovered, regenerated and reused, increasing the sustainable aspect of these processes.

Recently, we reported the behavior of metal oxides in the Cannizzaro reaction of pyruvaldehyde, the very last step in the cascade conversion from trioses.[25] It was shown that Lewis acid

sites are fundamental to the Cannizzaro reaction, while Brønsted sites play no role. In this contribution, we focus on the direct aqueous-phase cascade conversion of glyceraldehyde into lactic acid over some simple metal oxides (Nb_2O_5, TiO_2, ZrO_2 and SnO_2) in a fixed-bed flow reactor. Special attention is given to the water-tolerance of the catalyst surface acid sites. The acidity was characterized on both hydrated and dehydrated catalyst surfaces to monitor how the amount and the strength of the active sites change in presence of water.

Results

Catalysts Acid-Base Properties

Structural and textural properties of all commercial and synthesized catalysts were formerly investigated and the results are reported and discussed elsewhere.[25] It was shown that, apart from hydrated niobia (Nb_2O_5) and calcined Nb_2O_5-400 (89 $m^2 g^{-1}$), ZrO_2 (103 $m^2 g^{-1}$), TiO_2 (54 $m^2 g^{-1}$) and SnO_2 (28 $m^2 g^{-1}$) are all crystalline powders. ZrO_2 presents essentially a monoclinic structure (96%), while TiO_2 is characterized by its anatase phase (83%). Total acidity was also previously determined by titration in aqueous medium, and it was found that SnO_2 exhibits the lowest concentration of acid sites (1100 mol g^{-1}) while Nb_2O_5 holds the highest (4700 mol g^{-1}), which decreased around 40% after thermal treatment (Nb_2O_5, 2800 mol g^{-1}). ZrO_2 and TiO_2 had similar concentrations of acid sites (3000 and 2900 mol g^{-1}).[25] Even though such assessment was successfully correlated to catalyst activity in Cannizzaro reaction, it does not allow to discuss the nature and the strength of acid sites. Furthermore, the impact of the well-known interaction of water with surface acid centers cannot be assessed either, limiting any further discussion on the role of each site in aqueous-phase reactions. Therefore, in this current contribution the characterization of acid-base properties was expanded to address such issues.

The acidity of different metal oxides was initially investigated by monitoring pyridine adsorption with infrared spectroscopy. FTIR spectra of pyridine adsorbed on dehydrated catalysts are depicted in Figure 1a–c. Dehydrated Nb_2O_5 (Figure 1a) displayed absorption bands at ~1445, 1575 and 1608 cm^{-1}, which are typically assigned to pyridine coordinated to Lewis acid sites,[53,54] while the band recorded at ~1540 cm^{-1} reveals the presence of Brønsted acid sites, since this vibration corresponds to the formed pyridinium ions.[53,54] On the other

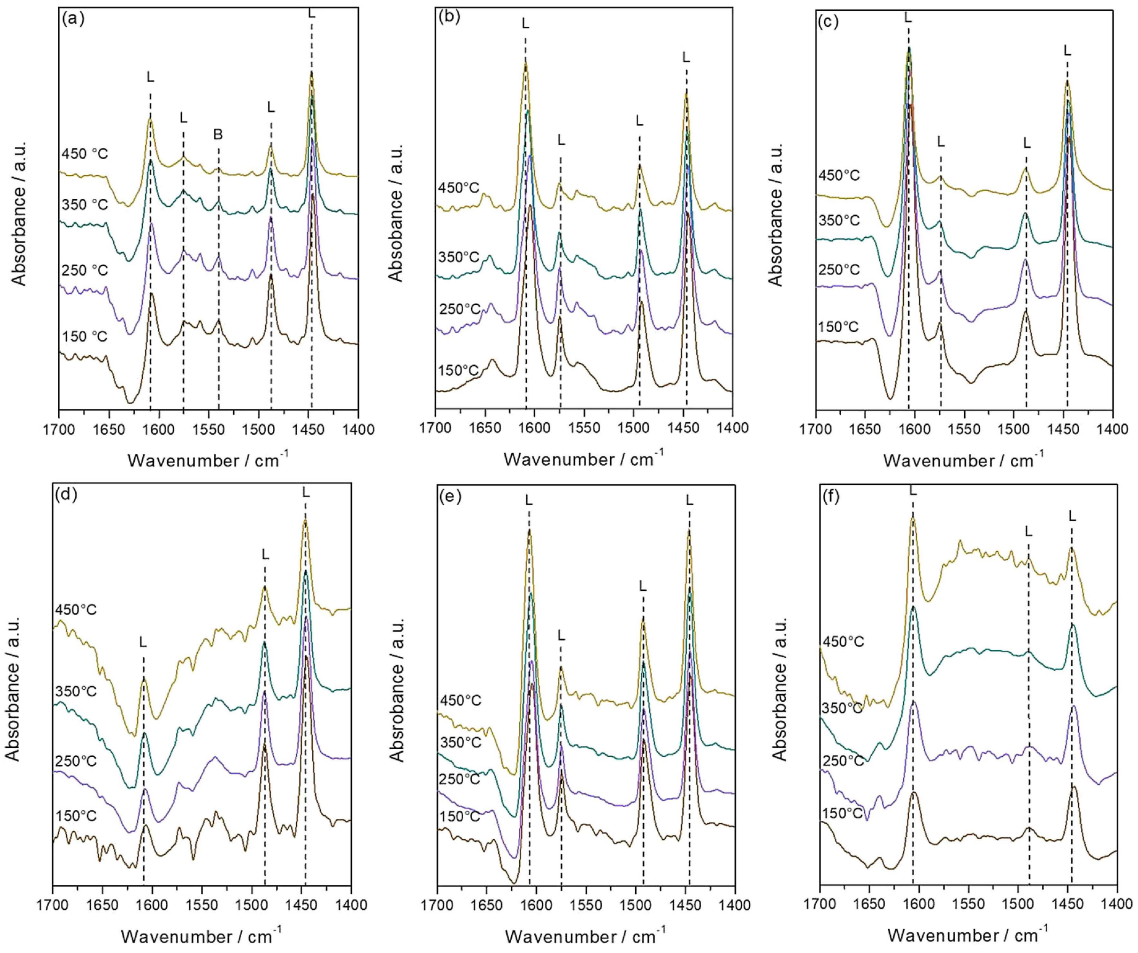

Figure 1. FTIR of dehydrated (a) Nb_2O_5, (b) TiO_2 and (c) ZrO_2 and hydrated (d) Nb_2O_5, (e) TiO_2 and (f) ZrO_2.

hand, the other catalysts (TiO_2 and ZrO_2) exhibit only those bands related to Lewis acid sites (Figure 1b,c). No adsorbed pyridine spectra could be collected for SnO_2 since pyridine was completely desorbed from the oxide surface as soon as the sample was evacuated (Figure S1).

Performing pyridine adsorption in the presence of water (Figure 1d–f) revealed that all the bands associated with Lewis acid sites are still present in the samples spectra, indicating the existence of water-tolerant Lewis acid sites in all three catalysts. The density of all acid sites is summarized in Table 1.

Table 1. Concentration of Brønsted and Lewis acid sites and water-tolerant Lewis acid sites, and selectivities to propene ($S_{Propene}$) and acetone ($S_{Acetone}$) from isopropanol decomposition over all catalysts at 240 °C.

Catalyst	Brønsted acid sites [μmol g^{-1}]	Lewis acid sites [μmol g^{-1}]	Water-tolerant Lewis acid sites [μmol g^{-1}]	$S_{Propene}$ [%]	$S_{Acetone}$ [%]
Nb_2O_5	9	81	31	100	–
TiO_2	–	47	22	94	6
ZrO_2	–	79	5	90	10
SnO_2	–	–	–	6	94

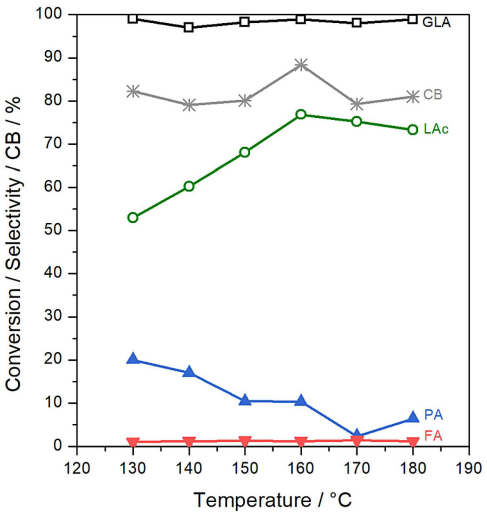

Figure 2. Evolution of glyceraldehyde conversion and selectivity to pyruvaldehyde (PA), lactic acid (LAc) and formaldehyde (FA), and carbon balance (CB) over Nb_2O_5 as a function of reaction temperature. Conditions: 10 bar, flow of 0.3 mL min^{-1} and W/F = 1 g min mL^{-1}. Data were collected after 1 h on stream.

On both hydrated and dehydrated catalysts, the bands at ~1450 cm^{-1} (Lewis acid sites) were registered even after desorption at 450 °C under vacuum. Their intensities decreased though, because only a fraction of the acid sites was strong enough to bind pyridine in vacuum at elevated temperature.

Isopropanol decomposition was used as a typical model reaction to estimate the catalysts acid-base surface properties.[55–57] Dehydrogenation of isopropanol leads to the formation of acetone and hydrogen, while dehydration produces propene and water. The first pathway has been related to the basicity of a solid, whereas the dehydration reaction, which occurs over acid sites, is associated to the acidity of oxides.[55–57] Table 1 summarizes the results obtained for isopropanol decomposition reaction over all the studied catalysts. The selectivities to propene and acetone, the two main products of the possible parallel reactions, summed up to 100% for all samples.

Over Nb_2O_5, isopropanol was solely converted to propene. In contrast, TiO_2, ZrO_2 and SnO_2, produced both propene and acetone. Nevertheless, TiO_2 and ZrO_2 drove the conversion of isopropanol mainly to propene, with selectivities of more than 90%, whilst the formation of acetone was much more significant (94%) over SnO_2.

Catalytic Activity and Stability

In a first experiment, the temperature effect on the continuous aqueous-phase transformation of glyceraldehyde was assessed by monotonically increasing the temperature from 130 °C to 180 °C. This preliminary assessment was performed over Nb_2O_5 catalyst, and lactic acid, pyruvaldehyde and formaldehyde were the main products identified, accounting for around 80–95% of the carbon balance.

The temperature increase mainly affects the product selectivities with no relevant impact on carbon balance up to 160 °C (Figure 2). Lactic acid selectivity steadily increased with increasing temperature, reaching the highest value of ~75% at 160 °C, exhibiting a drop at higher temperature. Pyruvaldehyde was the second major product, but its selectivity decreased from 30% to around 10% within the temperature range evaluated. Formaldehyde was also produced, but at a much lower concentration, resulting in selectivity values about 1–3%. The catalyst performance at 180 °C worsened because of the occurrence of degradation/polymerization side reactions. In fact, lactic acid and pyruvaldehyde selectivity dropped at high temperature.

All acid catalysts were then tested at 130 °C, and the time-dependent curves for glyceraldehyde conversion and selectivity to different products are depicted in Figure 3. Despite distinct activities, all catalysts were active to convert glyceraldehyde. Nb_2O_5 and ZrO_2 presented the highest conversions, while SnO_2 showed an initial conversion of ~90%, but dropped to 75% in the first 4 h of reaction. The least active catalyst was TiO_2 with an initial conversion of 75%, which progressively decreased to 65% over the time on stream. Besides the distinguished initial activities, these catalysts also showed different deactivation behavior.

The product distribution was also different for all catalysts (Figure 3). Nb_2O_5 presented higher selectivity to lactic acid, although it dropped with increasing time on stream, while pyruvaldehyde selectivity increased (Figure 3a). No other product was formed with significant concentration as only traces of formaldehyde were detected. TiO_2 exhibited a similar behavior with an initial high lactic acid selectivity that decreased with time on stream, while pyruvaldehyde production gradually increased (Figure 3b). However, a more significant formation of

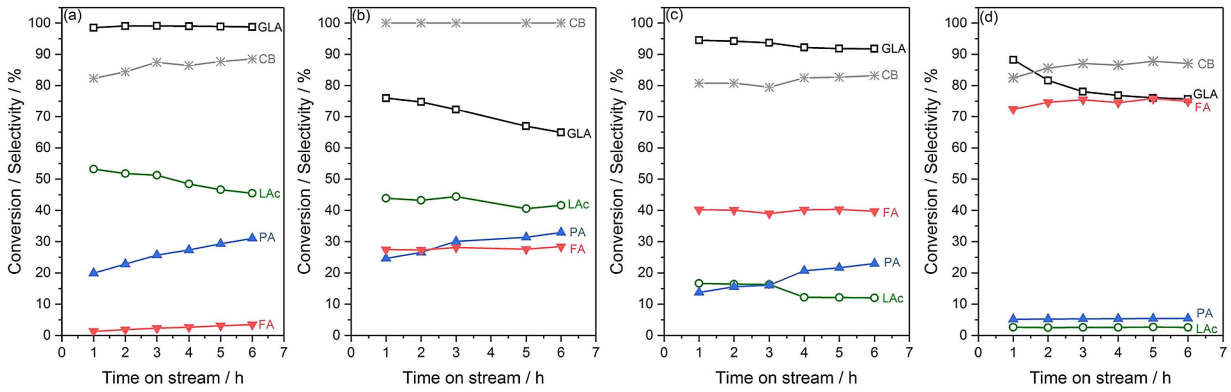

Figure 3. Glyceraldehyde conversion, products selectivity to lactic acid (LAc), pyruvaldehyde (PA) and formaldehyde (FA), and carbon balance (CB) evolution obtained for (a) Nb_2O_5, (b) TiO_2, (c) ZrO_2 and (d) SnO_2. All reactions were performed at 130 °C, 10 bar, flow of 0.3 mL min^{-1} and W/F = 1 g min mL^{-1}.

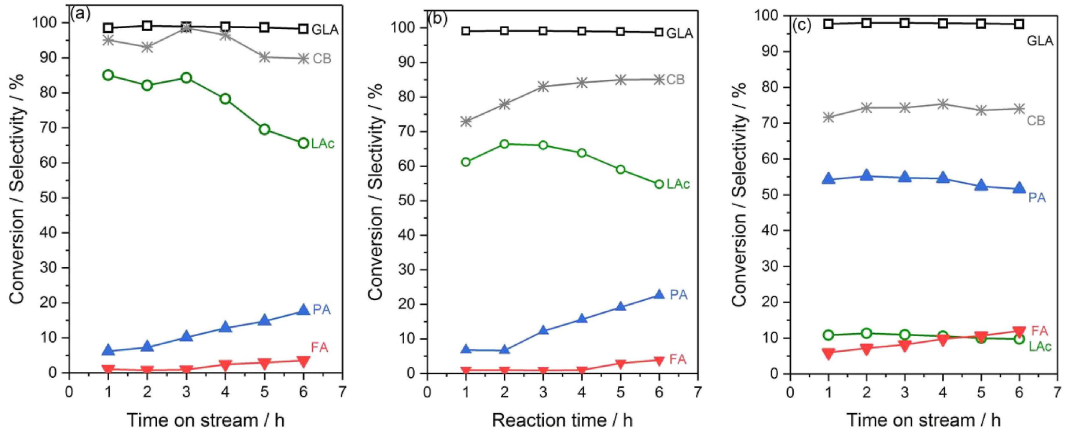

Figure 4. Glyceraldehyde conversion, products selectivity to lactic acid (LAc), pyruvaldehyde (PA) and formaldehyde (FA), and carbon balance (CB) evolution obtained for (a) Nb_2O_5, (b) Nb_2O_5-400 and (c) Amberlyst 35. All reactions were performed at 160 °C, 10 bar, flow of 0.3 mL min^{-1} and W/F = 1 g min mL^{-1}.

formaldehyde was noticed, outlining an important distinction in product distribution between TiO_2 and Nb_2O_5. The performance of ZrO_2 was even more distinct, since formaldehyde was the main product obtained with a steady selectivity of 40% over the whole reaction period monitored. However, like TiO_2 and Nb_2O_5, ZrO_2 showed a decrease in lactic acid selectivity along with an increase in pyruvaldehyde selectivity with time on stream (Figure 3c). Finally, formaldehyde was essentially the only reaction product formed over SnO_2 (Figure 3d), since the selectivities towards lactic acid and pyruvaldehyde did not surpass ~5% in line with a previous report of aqueous-phase conversion of dihydroxyacetone into lactic acid.[26]

Glyceraldehyde conversion was also carried out at 160 °C over Nb_2O_5 to examine the dynamics of lactic acid formation at higher temperatures. This catalyst was selected since it showed the most promising performance among the catalysts studied here. The time-resolved conversion and selectivity curves displayed in Figure 4a show a behavior similar to that observed for Nb_2O_5 catalyst at 130 °C. Lactic acid was the main product with 85% selectivity up to 3 h on stream, after its selectivity started decreasing while the pyruvaldehyde one started increasing. These changes were much more pronounced than the corresponding ones at 130 °C (Figure 3a). Only a very low concentration of formaldehyde was formed. These product distribution patterns were found to be alike no matter the reaction temperature or the temperature at which Nb_2O_5 was thermally treated. Indeed, lactic acid formation at 160 °C over Nb_2O_5-400 (Figure 4b) was lower than that obtained on Nb_2O_5 at the same reaction temperature (Figure 4a) but higher than that accomplished over Nb_2O_5 when the reaction was carried out at 130 °C (Figure 3a). For the sake of comparison, these curves are compared in Figure S2.

The poorer product distribution of Nb_2O_5-400 at 160 °C could be related to a lower density of Brønsted acid sites, since it is well known that their density gradually diminishes when hydrated Nb_2O_5 is calcined.[52,58] Therefore, a catalyst containing only Brønsted acid sites, Amberlyst 35, was tested to fully understand their importance for the reaction pathway, and the results are shown in Figure 4c. Pyruvaldehyde was the main product with a steady selectivity of ~55%. Lactic acid was produced with selectivity of only ~10%. It should be noted that the carbon balance was the lowest among all catalysts studied, 70–75%.

Discussion

Processes for conversion of biomass-derived oxygenates are expected to be performed in the liquid phase since the vapor pressure of these molecules is typically very low. Water is the most convenient solvent and thus the interaction of water molecules with the catalyst surface is very relevant.[49,59] This is particularly true when acid-catalyzed reactions are involved as there are usually different possible reaction pathways from an oxygenate compound that can be promoted on acid sites. Therefore, acid-catalyzed conversion of oxygenates in water strongly depends on differences of the nature of the acid sites, turning the discussion on catalyst acidity quite important.

Data collected from infrared spectra of adsorbed pyridine and isopropanol decomposition evidenced that the catalysts studied herein possess very different acidity in terms of three important properties: type, strength and tolerance to water. Nb_2O_5 contains both Lewis and Brønsted acid sites that are well characterized by the absorption bands at around 1446 and 1540 cm^{-1} in the infrared spectra of adsorbed pyridine/pyridinium ions, while only Lewis acidity is present in the other metal oxides, as expected.[54,58] The observation of bands ascribed to pyridine adsorbed on Lewis acid sites of metal oxides that were saturated with water illustrates that such sites are still active despite the expected formation of stable Lewis acid-water adducts. The susceptibility of the Lewis acid sites on these different oxides to water was obvious though, as indicated by the differences in the fraction of water-tolerant Lewis acid sites (Table 1). TiO_2 showed the highest fraction of water-tolerant Lewis acid sites (47%), closely followed by Nb_2O_5 (40%). ZrO_2 revealed to be very sensitive to water, containing only ~6% of water-tolerant Lewis acid sites, while most of them are unable to adsorb pyridine under 'wet' conditions. While it is possible that pyridine and biomass-derived oxygenates are affected by competition with water in different ways, these results are at least a qualitative metric for the water-tolerance of Lewis acid sites. Similar observations were reported in the literature for some of the same metal oxide catalysts.[52,60] However, the fraction of water-tolerant Lewis acid sites on Nb_2O_5 and TiO_2 determined in these contributions differs from those reported before.[52,60] These differences are likely attributed to the synthesis procedures of the metal oxides, leading to distinct structural and textural properties. Indeed, it was shown that the fraction of water-tolerant Lewis acid sites on an amorphous and a large surface area, defect-rich orthorhombic Nb_2O_5 is different.[35] Distinct experimental procedures may also contribute for these different results.

In addition, isopropanol decomposition indicated noticeable differences in the acid-base properties among the different catalysts. The acid-base properties of Nb_2O_5 are defined by its acid sites since propene was essentially the only product formed (Table 1). Over TiO_2, ZrO_2 and SnO_2, simultaneous dehydration and dehydrogenation reactions took place, producing both propene and acetone, indicating that on these catalysts, both acid and base sites play a kinetically significant role. However, the high selectivity to acetone (94%) over SnO_2 shows that reactions over basic surface sites dominate over this catalyst.

The catalysts were investigated in the aqueous-phase conversion of glyceraldehyde, a three-carbon monosaccharide commonly found as an intermediate during the conversion of glycerol, hexoses, or pentoses in biorefining processes. Glyceraldehyde can be converted to lactic acid through a cascade reaction starting with its dehydration to pyruvaldehyde. In the second step, a water molecule is added to pyruvaldehyde, and a rearrangement occurs (Scheme 1). No triose conversion is expected to proceed without a catalyst.[27,34]

The first reaction step – glyceraldehyde dehydration – is favored over Nb_2O_5 at even the lowest temperature used. It was seen that lactic acid is the main product at 130 °C and its production is pushed up as temperature rises (Figure 2). The concomitant drop in pyruvaldehyde selectivity evidences that the Cannizzaro reaction in the end of the cascade reaction path is accelerated. Albuquerque *et al.*[24] have indeed shown that pyruvaldehyde rearrangement to lactic acid is improved at high temperature. At elevated temperature, side reactions contribute more significantly to the conversion of glyceraldehyde (Figure 2), in particular, when the temperature increased to 180 °C. Indeed, the decrease of both lactic acid and pyruvaldehyde selectivity (Figure 2) suggests that high molecular weight compounds or carbonaceous deposits are formed with increasing temperature.

Comparing all catalysts at 130 °C revealed different behavior, as shown by the time-dependent conversion curves depicted in Figure 3. These performances are likely associated with the type of acid sites on these catalysts. In the literature it is reported that dehydration of monosaccharides is generally kinetically favored in the presence of Brønsted acid sites, though it can also proceed on Lewis acid-base site pairs.[61] Nb_2O_5 was the only catalyst with Brønsted acidity used in this study (Figure 1a), and it was indeed the most active catalyst. The high activity of Brønsted acid centers in dehydrating glyceraldehyde was also illustrated by using Amberlyst 35 as catalyst in a control experiment, in which glyceraldehyde was fully converted into pyruvaldehyde (Figure 3c). These findings are also in line with the seminal work of Lookhart and Feather on trioses dehydration in the presence of H_2SO_4 as a homogeneous Brønsted acid catalyst.[62] Nevertheless, the formation of pyruvaldehyde over TiO_2 and ZrO_2 shows that dehydration of glyceraldehyde can also take place on the less active Lewis centers. A contribution of Brønsted sites generated by enhanced water dissociation following the interaction of hydroxyl ions from water molecules with the exposed coordinatively unsaturated cationic sites (Lewis centers) is also conceivable. This modification of the intrinsic nature of acid surface sites due to hydration effects when a catalyst works in water is an issue of major interest for biomass conversion processes that requires further attention.[59,63,64]

The different product distribution noted when comparing all catalysts at 130 °C (Figure 3) can be also ascribed to the differences in the nature of their acid sites. As reaction is carried out in water, the annihilation of Lewis acidity by irreversible formation of water-Lewis acid adduct is a major concern.

Essentially only those sites that can maintain their Lewis acidity, the so-called water-tolerant Lewis acid sites, can promote the acid-catalyzed Cannizzaro cascade step producing lactic acid. Therefore, the efficiency of a catalyst would be expected to be determined mostly by the amount of active water-tolerant Lewis acid sites on its surface. One should bear in mind though that the activity of water-tolerant Lewis acid sites will also be defined by the nature of the oxygenate molecule being converted. Copeland et al.[65,66] studied the competitive adsorption of oxygenates with water on metal oxides and showed that the structure of the oxygenate molecule – carbon chain size and type, number and position of functional groups – can alter its interaction strength with the solid surface and its ability to replace water on surface sites. Water molecules (Lewis base) in the water-Lewis acid adducts can be displaced from the acid sites by a more basic oxygenate molecule, rendering an active Lewis acid site. In addition, there could be an entropic driving force when multiple water molecules are replaced by a single oxygenate molecule on a surface site.[49]

The formation of lactic acid decreased in the order Nb_2O_5 (53%) > TiO_2 (44%) > ZrO_2 (16%), and being negligible over SnO_2. Taarning et al.[26] also reported that SnO_2, either as nanopowder or supported on siliceous beta zeolite, was inactive for lactic acid production from dihydroxyacetone in water. This trend of lactic acid selectivity can be correlated to the concentration of water-tolerant Lewis acid sites on the catalysts studied here (Figure 5), evidencing that these sites are

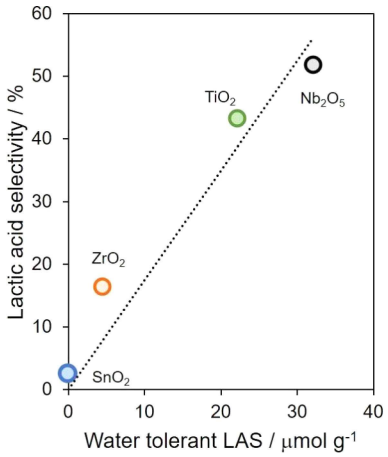

Figure 5. Correlation between lactic acid selectivity after 2 h on stream and water tolerant Lewis acid sites at 150 °C.

indeed required for the final Cannizzaro reaction step. Despite the co-existence of Brønsted acidity on Nb_2O_5, their contribution to the activity for the Cannizzaro reaction appear to be limited, since only small amounts of lactic acid were formed over solely Brønsted acidic Amberlyst 35 (Figure 4c) in line with previous studies focused specifically on pyruvaldehyde Cannizzaro reaction into lactic acid.[25]

The significant production of formaldehyde over the catalysts with no or low concentration of water-tolerant acid sites, SnO_2 and ZrO_2, demands some attention as well. Formaldehyde has not been observed as a product in pyruvaldehyde conversion at this reaction temperature,[24,25] and thus, the reaction pathway leading to it could start as a sequential reaction from lactic acid or as a parallel reaction path for glyceraldehyde conversion. No conversion was observed at all over these two catalysts when lactic acid was used as starting material under the same reaction conditions (130 °C, 10 bar, flow of 0.3 mL min^{-1} and W/F = 1 g min mL^{-1}) in a control experiment (Figure S3). Similar results were previously reported on a H-USY zeolite catalyst.[27] These findings show that lactic acid is neither further transformed to other chemicals over ZrO_2 and SnO_2 nor reverse reaction takes place, substantiating the conclusion that formaldehyde is being produced from glyceraldehyde molecule cleavage.

Contrasting the behavior of the metal oxide catalysts in glyceraldehyde conversion with isopropanol decomposition results, it is possible to note that the production of formaldehyde correlates well with the formation of acetone (indicative of basic sites[55–57]), whereas the production of lactic acid correlates to the production of propene (associated with the acidic sites[55–57]) from isopropanol (Figure 6). These results

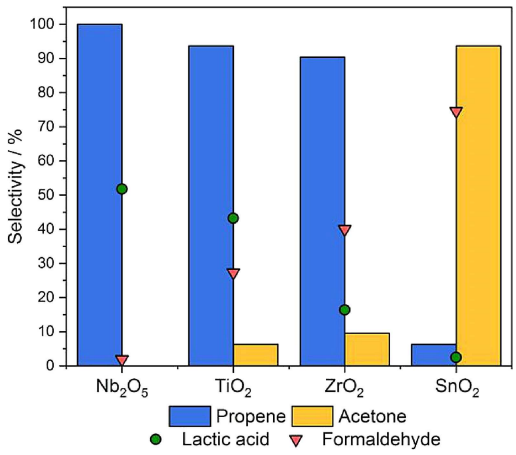

Figure 6. Correlation between propene and acetone formation from isopropanol decomposition and lactic acid and formaldehyde production from glyceraldehyde transformation.

support the conclusion that formaldehyde selectivity is determined by the existence of relevant surface basic sites, which promote C–C cleavage in the glyceraldehyde molecule. On the other hand, lactic acid selectivity increased along with propene formation, corroborating the previous discussion that lactic acid production is driven by the catalyst acidity, more specifically the water-tolerant Lewis acid sites as shown in Figure 5.

The reaction mechanism of the cascade transformation of glyceraldehyde could thus be rationalized as involving two steps with pyruvaldehyde as the intermediate as proposed before.[26,29,67] The first step is claimed to involve a keto-enol tautomerization followed by dehydration promoted by both Brønsted and Lewis acid sites.[67,68] Pyruvaldehyde is then

rearranged to lactic acid via a hydride-shift mechanism with addition of a water molecule on Lewis acid sites.[24,25,67,68]

The Nb_2O_5 catalyst presented the highest lactic acid formation but also showed a decline on its selectivity, while the pyruvaldehyde yield increased with increasing time on stream (Figure 4a). This behavior suggests that the water-tolerant Lewis acid sites catalyzing the second cascade step – transformation of pyruvaldehyde into lactic acid – might be suffering from some deactivation. The performance of TiO_2, the second best performing catalyst concerning lactic acid selectivity (Figure 3b), corroborates this suggestion. Since the water-tolerant Lewis acid sites have activity for both glyceraldehyde dehydration and the Cannizzaro reaction of pyruvaldehyde over this metal oxide, the deactivation of such sites impacts both lactic acid selectivity and glyceraldehyde conversion. As for ZrO_2 and SnO_2, the base sites are likely the ones more affected by deactivation. Deactivation is probably caused by the blockage of surface sites upon formation of carbonaceous compounds as reported elsewhere.[26,27]

A regeneration test was then performed with TiO_2. The spent catalyst was collected after the first 6 h on stream, calcined at 500 °C and a new run was carried out. The catalyst activity was recovered as seen in Figure 7, corroborating the suggestion that deactivation is likely associated with carbonaceous deposits. Indeed similar conversion patterns were observed for both fresh and regenerated catalysts within the whole period of 6 h on stream (Figure S4).

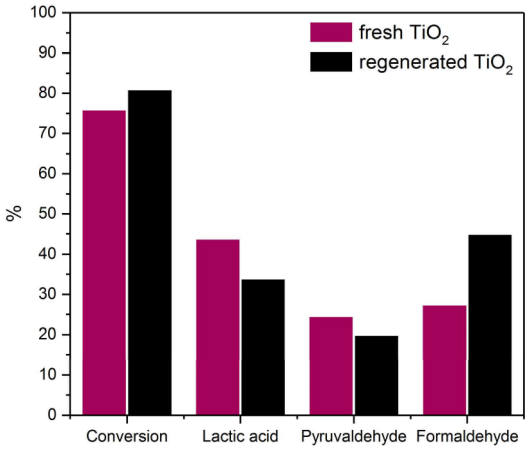

Figure 7. Comparison of the catalytic performance of fresh and regenerated TiO_2. Conditions: 10 bar, flow of 0.3 mL min^{-1} and W/F = 1 g min mL^{-1}. Data compared after 1 h on stream.

A decrease in lactic acid and pyruvaldehyde selectivities along with a proportional increase in formaldehyde was noticed though. This disturbance in product selectivity might be related to the activation of more basic sites of TiO_2 upon calcination at such high temperature (500 °C).

Conclusions

It was shown that transformation of glyceraldehyde into lactic acid proceeds via a cascade reaction, in which glyceraldehyde is initially dehydrated to pyruvaldehyde, followed by the Cannizzaro reaction that involves the addition of a water molecule and molecular rearrangement to lactic acid. The dehydration step is claimed to occur on Brønsted acid sites and/or on water-tolerant Lewis acid sites. These later sites also determine the selectivity to lactic acid. Nb_2O_5 and TiO_2 were the metal oxide catalysts holding the largest fractions of water-tolerant Lewis acid sites, rendering them more selective catalysts. Nb_2O_5, however, is a more promising system due to the synergy between its Brønsted acid sites, which promote the first cascade step, and the water-tolerant Lewis acid sites that catalyze the final Cannizzaro reaction. The presence of strong base sites promotes glyceraldehyde fragmentation to formaldehyde with high selectivity.

All in all, the results shown herein reveal that a good catalyst for direct aqueous-phase conversion of glyceraldehyde to lactic acid should have the right ratio of Brønsted and water-tolerant Lewis acid sites to assist each reaction step and avoid the presence of strong base sites.

Experimental Section

Catalysts

Commercial ZrO_2 (Saint Gobain Norpro), TiO_2 (Evonik) and $Nb_2O_5 \cdot nH_2O$ (CBMM) oxides were used in this work. $Nb_2O_5 \cdot nH_2O$ was used both without any treatment, i.e. as niobic acid hereinafter labeled simply as Nb_2O_5, and after calcination in a muffle at 400 °C (Nb_2O_5-400) following a heating rate of 10 °C min^{-1} for 4 h. All oxides were ground and sieved to obtain particles size ranging between 53 and 63 μm to avoid any effect of mass transfer limitations.[24]

Complementarily, a commercial Amberlyst 35 (Rohm and Haas) was also tested as Brønsted acid catalyst, and a SnO_2 was synthesized in the laboratory by precipitation.[25] An aqueous solution of $SnCl_4 \cdot 5H_2O$ at 0.25 mol L^{-1} was used as tin precursor and a NH_4OH solution (0.32 mol L^{-1}) was taken as precipitating agent. Synthesis was carried out at room temperature. The resulting solid was recovered by centrifugation, washed with water and dried at 100 °C overnight. Lastly, it was calcined at 500 °C (10 °C min^{-1}) for 4 h.

Catalysts Acid-Base Properties

Acidity was assessed by Fourier Transform Infrared Spectroscopy using pyridine as probe molecule (FTIR-Py) on both dehydrated and hydrated catalysts surfaces. The experiments were performed using a Nicolet 8700 FTIR spectrometer with an MCT/A detector. Each dehydrated sample was loaded into a vacuum transmission cell as self-supported wafer (diameter 1.25 cm). The sample was activated at 450 °C for 1 h under high vacuum. A background spectrum was recorded at 150 °C. Then, 0.1 mbar of pyridine was dosed in the cell for 30 min. Subsequently, the cell was evacuated for 1 h to remove physisorbed pyridine. To determine the strength of acid sites a temperature programmed desorption was carried out. The sample was heated to 250, 350 and 450 °C for 1 h, and each spectrum was taken at 150 °C. In contrast, the hydrated surface was obtained by

exposing the sample to ambient air for 2 days before pressing the wafer. Then, the catalyst wafer was kept in contact with the atmosphere for 5 h before loading it into the transmission cell. In this case, the sample was not pretreated before running the infrared spectroscopy experiment, which was carried out as reported for the dehydrated sample. Brønsted and Lewis acid sites concentration was determined by Lambert-Beer equation [Eq. (1)]:

$$C_w = \frac{A_{peak} \times S}{W \times \varepsilon} \quad (1)$$

Where C_w ($\mu mol\,g^{-1}$), W (g), S (cm^2) and ε ($cm^2\,\mu mol^{-1}$) indicate weight-based concentration, sample mass, sample disk area and integrated molar extinction coefficient as reported by Tamura et al.[69]

In addition, the acid-base properties of the catalysts were evaluated by isopropanol decomposition.[55–56] Experiments were carried out in a fixed-bed glass reactor at 240 °C at atmospheric pressure and under differential conditions ($\leq$ 15 %). Isopropanol was admitted into the reactor with the aid of a saturator kept at 10 °C and a flow of nitrogen. Isopropanol conversion and the formation of acetone and propane were monitored online by gas chromatography in an Agilent 6850A equipped with a flame ionization detector. Acidity and basicity were inferred by the selectivities to propene and acetone, respectively.[55–56]

Catalytic Activity

Catalytic conversion of glyceraldehyde was performed in a fixed bed up-flow reactor (160 mm long and 6.35 mm i.d.). To keep the catalyst bed in place, glass wool was used in both ends of the reactor. The reactor was packed with 0.3 g of catalyst (53–63 μm). A glyceraldehyde aqueous solution at 0.22 $mol\,L^{-1}$ was pumped by a Gilson 307 HPLC pump with a flow rate of 0.3 $mL\,min^{-1}$. The pressure was set at 10 bar using a Swagelok back pressure regulator and the preheater and reactor temperature was set at the desired temperature. Reaction samples were collected for products analysis at various times on stream.

Glyceraldehyde and product concentrations were monitored and quantified by high performance liquid chromatography (HPLC) in Waters Alliance e2695 equipped with a refractive index detector (RID) kept at 50 °C and a photodiode array detector (PDA). A Biorad Aminex HPX-87H ion exchange column was used at 65 °C in isocratic elution mode (0.7 $mL\,min^{-1}$) with a 5 $mmol\,L^{-1}$ H_2SO_4 solution as mobile phase. Before injecting in the chromatograph, samples were filtered using 0.22 μm PVDF filter. Quantification was done based on calibration curves ($R^2 > 0.999$) constructed using aqueous solutions of standards of all identified organic compounds. All liquid samples were analyzed in triplicate and the data are reported as the mean values. The calculated error was < 2 %.

Glyceraldehyde conversion (X_G), products selectivity (S) and carbon balance (CB) were determined by [Eq. (2)–(4)]:

$$X_{GLA} = \frac{(C_{GLA_0} - C_{GLA_t})}{C_{GLA_0}} \times 100\,\% \quad (2)$$

$$S = \frac{nC_P}{n \times (C_{GLA_0} - C_{GLA_t})} \times 100\,\% \quad (3)$$

$$CB = \frac{nC_{GLA_t} + \sum nC_P}{nC_{GLA_0}} \times 100\,\% \quad (4)$$

Where C_{GLA_0} is glyceraldehyde initial concentration, C_{GLA_t} is glyceraldehyde concentration at the time samples were collected, t, C_P is product concentration and n is the number of carbon atoms in the chemical molecule.

Acknowledgements

The authors acknowledge the financial support from CNPq (Brazil). K.M.A.S. also acknowledges CAPES/Embrapa (Brazil) for the scholarship. E.M.A. thanks PCI/CNPq (Proc. 313014/2016-7) for her postdoctoral grant. Financial support from the U.S. Nation Science Foundation (grant number: CBET-1705444) is gratefully acknowledged.

Conflict of Interest

The authors declare no conflict of interest.

Keywords: glyceraldehyde · biomass conversion · water-tolerant acid sites · Cannizzaro reaction · dehydration

[1] A. Mansouri, R. Rihani, A. N. Laoufi, M. Özkan, *Fuel* **2016**, *185*, 612–621.
[2] P. Gallezot, *Chem. Soc. Rev.* **2012**, *41*, 1538–1558.
[3] M. Hajjari, M. Tabatabaei, M. Aghbashlo, H. Ghanavati, *Renewable Sustainable Energy Rev.* **2017**, *72*, 445–464.
[4] F. Ma, M. A. Hanna, *Bioresour. Technol.* **1999**, *70*, 1–15.
[5] A. E. Atabani, A. S. Silitonga, I. A. Badruddin, T. M. I. Mahlia, H. H. Masjuki, S. Mekhilef, *Renewable Sustainable Energy Rev.* **2012**, *16*, 2070–2093.
[6] C. H. Zhou, J. N. Beltramini, Y. X. Fan, G. Q. Lu, *Chem. Soc. Rev.* **2008**, *37*, 527–549.
[7] Y. Li, M. Nielsen, B. Li, P. H. Dixneuf, H. Junge, M. Beller, *Green Chem.* **2015**, *17*, 193–198.
[8] A. Villa, N. Dimitratos, C. E. Chan-Thaw, C. Hammond, L. Prati, G. L. Hutchings, *Acc. Chem. Res.* **2015**, *48*, 1403–1412.
[9] H. R. Safaei, M. Shekouhy, S. Rahmanpur, A. Shirinfeshan, *Green Chem.* **2012**, *14*, 1696–1704.
[10] M. D. González, P. Salagre, R. Mokaya, Y. Cesteros, *Catal. Today* **2014**, *227*, 171–178.
[11] G. M. Lari, G. Pastore, M. Haus, Y. Ding, S. Papadokonstantakis, C. Mondelli, J. Pérez-Ramírez, *Energy Environ. Sci.* **2018**, *11*, 1012–1029.
[12] B. Katryniok, H. Kimura, E. Skrzynska, J. S. Girardon, P. Fongarland, M. Capron, R. Ducoulombier, N. Mimura, S. Paul, F. Dumeignil, *Green Chem.* **2011**, *13*, 1960–1979.
[13] S. C. D'Angelo, A. Dall'Ara, C. Mondelli, J. Pérez-Ramírez, S. Papadokonstantakis, *ACS Sustainable Chem. Eng.* **2018**, *6*, 16563–16572.
[14] P. Mäki-Arvela, I. L. Simakova, T. Salmit, D. Y. Murzin, *Chem. Rev.* **2014**, *114*, 1909–1971.
[15] T. Miyazawa, S. Koso, K. Kunimori, K. Tomishige, *Appl. Catal. A* **2007**, *329*, 30–35.
[16] H. H. C. M. Pinxt, B. F. M. Kuster, G. B. Marin, *Appl. Catal. A* **2000**, *191*, 45–54.
[17] A. Kinage, P. P. Upare, P. Kasinathan, Y. K. Hwang, J. S. Chang, *Catal. Commun.* **2010**, *11*, 620–6223.
[18] E. M. Albuquerque, L. E. P. Borges, M. A. Fraga, *J. Mol. Catal. A* **2015**, *400*, 64–70.
[19] E. M. Albuquerque, L. E. P. Borges, M. A. Fraga, *Green Chem.* **2015**, *17*, 3889–3899.
[20] E. G. Rodrigues, M. F. R. Pereira, J. J. Delgado, Z. Chen, J. J. M. Órfão, *Catal. Commun.* **2011**, *16*, 64–69.

[21] G. M. Lari, C. Mondelli, J. Pérez-Ramírez, *ACS Catal.* **2015**, *5*, 1453–1461.
[22] D. Hekmat, R. Bauer, J. Fricke, *Bioprocess Biosyst. Eng.* **2003**, *26*, 109–116.
[23] G. M. Lari, R. Garcia-Muelas, C. Mondelli, N. López, J. Pérez-Ramírez, *Green Chem.* **2016**, *18*, 4682–4692.
[24] E. M. Albuquerque, L. E. P. Borges, M. A. Fraga, C. Sievers, *ChemCatChem* **2017**, *9*, 2675–2683.
[25] K. M. A. Santos, E. M. Albuquerque, L. E. P. Borges, M. A. Fraga, *Mol. Catal.* **2018**, *458*, 198–205.
[26] E. Taarning, S. Saravanamurugan, M. S. Holm, J. Xiong, R. M. West, C. H. Christensen, *ChemSusChem* **2009**, *2*, 625–627.
[27] R. M. West, M. S. Holm, S. Saravanamurugan, J. Xiong, Z. Beversdorf, E. Taarning, C. H. Christensen, *J. Catal.* **2010**, *269*, 122–130.
[28] K. P. F. Janssen, J. S. Paul, B. F. Sels, P. A. Jacobs, *Stud. Surf. Sci. Catal.* **2007**, *170*, 1222–1227.
[29] P. P. Pescarmona, K. P. F. Janssesn, C. Delaet, C. Stroobants, K. Houthoofd, A. Philippaerts, C. D. Jonghe, J. S. Paul, P. A. Jacobs, B. F. Sels, *Green Chem.* **2010**, *12*, 1083–1089.
[30] H. J. Cho, P. Dornath, W. Fan, *ACS Catal.* **2014**, *4*, 2029–2037.
[31] L. Li, C. Stroobants, K. Lin, P. A. Jacobs, B. F. Sels, P. P. Pescarmona, *Green Chem.* **2011**, *13*, 1175–1181.
[32] J. Wang, Y. Masui, M. Onaka, *Appl. Catal. B* **2011**, *107*, 135–139.
[33] A. M. Mylin, S. I. Levytska, M. E. Sharanda, V. V. Brei, *Catal. Commun.* **2014**, *47*, 36–39.
[34] E. Pighin, V. K. Díez, J. I. Di Cosimo, *Appl. Catal. A* **2016**, *517*, 151–160.
[35] K. Nakajima, J. Hirata, M. Kim, N. K. Gupta, T. Murayama, A. Yoshida, N. Hiyoshi, A. Fukuoka, W. Ueda, *ACS Catal.* **2018**, *8*, 283–290.
[36] F. de Clippel, M. Dusselier, R. V. Rompaey, P. Vanelderent, J. Dijkmans, E. Makshina, L. Giebeler, S. Oswaldt, G. V. Baron, J. F. M. Denayer, P. P. Pescarmona, P. A. Jacobs, B. F. Sels, *J. Am. Chem. Soc.* **2012**, *134*, 10089–10101.
[37] L. Li, F. Shen, R. L. Smith, X. Qi, *Green Chem.* **2017**, *19*, 76–81.
[38] P. N. Paulino, O. C. Reis, Y. F. Licea, E. M. Albuquerque, M. A. Fraga, *Catal. Sci. Technol.* **2018**, *8*, 4945–4956.
[39] P. Y. Dapsens, C. Mondelli, J. Pérez-Ramírez, *ChemSusChem* **2013**, *6*, 831–839.
[40] S. Lux, M. Siebenhofer, *Catal. Sci. Technol.* **2013**, *3*, 1380–1385.
[41] M. S. Holm, S. Saravanamurugan, E. Taarning, *Science* **2010**, *328*, 602–605.
[42] J. Duo, Z. Zhang, G. Yao, Z. Huo, F. Jin, *Catal. Today* **2016**, *263*, 112–116.
[43] Q. Guo, F. Fan, E. A. Pidko, W. N. P. van der Graaff, Z. Feng, C Li, E. J. M. Hensen, *ChemSusChem* **2013**, *6*, 1352–1356, 2013.
[44] A. Feliczak-Guzik, M. Sprynskyy, I. Nowak, B. Buszewski, *Catalysts* **2018**, *8*, 31–42.
[45] A. Feliczak-Guzik, M. Sprynskyy, I. Nowak, M. Jaroniec, B. Buszewski, *J. Colloid Interface Sci.* **2018**, *516*, 379–383.
[46] E. Pighin, V. K. Díez, J. I. Di Cosimo *Catal. Today* **2017**, *289*, 29–37.
[47] E. Pighin, J. I. Di Cosimo, V. K. Díez *Mol. Catal.* **2018**, *458*, 189–197.
[48] X. Wang, F. Liang, C. Huang, Y. Lia, B. Chen *Catal. Sci. Technol.* **2015**, *5*, 4410–4421.
[49] C. Sievers, Y. Noda, L. Qi, E. M. Albuquerque, R. M. Rioux, S. L. Scott, *ACS Catal.* **2016**, *6*, 8286–8307.
[50] Y. Koito, K. Nakajima, M. Kitano, M. Hara *Chem. Lett.* **2013**, *42*, 873–875.
[51] Y. Koito, K. Nakajima, R. Hasegawa, H. Kobayashi, M. Kitano, M. Hara *Catal. Today* **2014**, *226*, 198–203.
[52] K. Nakajima, Y. Baba, R. Noma, M. Kitano, J. N. Kondo, S. Hayashi, M. Hara, *J. Am. Chem. Soc.* **2011**, *133*, 4224–4227.
[53] W. Turek, J. Haber, A. Krowiak, *Appl. Surf. Sci.* **2005**, *252*, 823–827.
[54] G. Busca, *Catal. Today* **1998**, *41*, 191–206.
[55] A. Gervasini, A. Auroux, *J. Catal.* **1991**, *131*, 190–198.
[56] A. Ouquour, G. Coudurier, J. C. Vedrine, *J. Chem. Soc. Faraday Trans.* **1993**, *89*, 3151–3155.
[57] M. Ziolek, J. Kujawa, O. Saur, J. C. Lavalley, *J. Mol. Catal. A* **1995**, *97*, 49–55.
[58] G. S. Foo, D. Wei, D. S. Sholl, C. Sievers, *ACS Catal.* **2014**, *4*, 3180–3192.
[59] R. Weingarten, G. A. Tompsett, W. C. Conner Jr., G. W. Huber, *J. Catal.* **2011**, *279*, 174–182.
[60] K. Nakajima, R. Noma, M. Kitano, M. Hara, *J. Phys. Chem. C* **2013**, *117*, 16028–16033.
[61] V. Choudhary, S. Sandler, D. Vlachos, *ACS Catal.* **2012**, *2*, 2022–2028.
[62] G. L. Lookhart, M. S. Feather, *Carbohydr. Res.* **1978**, *60*, 259–265.
[63] R. Rinaldi, F. Schüth, *Energy Environ. Sci.* **2009**, *2*, 610–626.
[64] B. Kasprzyk-Horden, *Adv. Colloid Interface Sci.* **2004**, *110*, 19–48.
[65] J. R. Copeland, X.-R. Shi, D. S. Sholl, C. Sievers, *Langmuir* **2013**, *29*, 581–593.
[66] J. R. Copeland, I. A. Santillan, S. M. Schimming, J. L. Ewbank, C. Sievers, *J. Phys. Chem. C* **2013**, *117*, 21413–21425.
[67] Y. Hayashi, Y. Sasaki, *Chem. Commun.* **2005**, 2716–2718.
[68] C. B. Rasrendra, B. A. Fachri, I. G. B. N. Makertihartha, S. Adisasmito, H. J. Heeres, *ChemSusChem* **2011**, *4*, 768–777
[69] M. Tamura, K. Shimizu, *Appl. Catal. A* **2012**, *433*, 135–145.

Manuscript received: March 26, 2019
Revised manuscript received: May 8, 2019
Accepted manuscript online: May 20, 2019
Version of record online: ■■, ■■■

FULL PAPERS

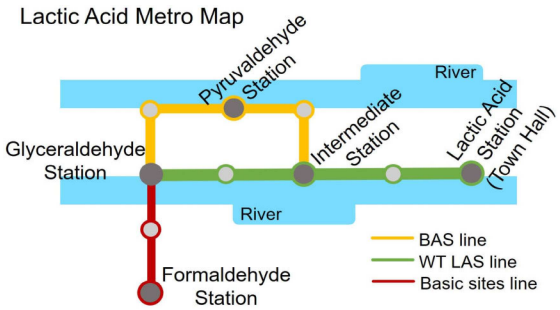

Next stop, Acid Sites: Acid-catalyzed conversion of trioses in water relies on differences in the nature of the acid sites.